Journal of The Electrochemical Society, **153** (2) A354-A360 (2006)
0013-4651/2005/153(2)/A354/7/$15.00 © The Electrochemical Society

Mixed Ionic–Electronic YSZ/Ni Composite for SOFC Anodes with High Electrical Conductivity

Fabio C. Fonseca,[a,z] Daniel Z. de Florio,[b] Vincenzo Esposito,[c,*] Enrico Traversa,[c,] Eliana N. S. Muccillo,[a,**] and Reginaldo Muccillo[a,**]**

[a]*Instituto de Pesquisas Energéticas e Nucleares, 05508-170 São Paulo, SP, Brazil*
[b]*Instituto de Química, UNESP, 14801-970 Araraquara, SP, Brazil*
[c]*Dipartimento di Scienze e Tecnologie Chimiche, Università degli Studi di Roma "Tor Vergata," 00133 Roma, Italy*

The preparation of the ZrO_2:8 mol % Y_2O_3/NiO (YSZ/NiO) composites by a modified liquid mixture technique is reported. Nanometric NiO particles dispersed over the yttria-stabilized zirconia (YSZ) were prepared, resulting in dense sintered specimens with no solid solution formation between the oxides. Such a feature allowed for the electrical characterization of the composites in a wide range of relative volume fraction, temperature, and oxygen partial pressure. The main results indicate that the composites have high electrical conductivity, and the transport properties in these mixed ionic-electronic (MIEC) composites are strongly dependent on the relative volume fraction of the phases, microstructure, and temperature. These parameters should hence be taken into consideration for the optimized design of MIEC composites for electrochemical applications. In this context, the composite was reduced under H_2 for the preparation of high-conductivity YSZ/Ni cermets for use as solid oxide fuel cell anode material with relatively low metal content.
 [DOI: 10.1149/1.2149312]

Manuscript submitted August 19, 2005; revised manuscript received October 3, 2005. Available electronically December 30, 2005.

Mixed ionic–electronic conductors (MIECs) have attracted a great deal of attention due to the variety of possible applications and interesting electrical properties.[1-3] These materials are thought to be used in high-temperature electrochemical devices such as gas separation membranes and solid oxide fuel cell (SOFC) electrodes.[2,3] The mixed conduction can be either an intrinsic property of single-phase materials (like cerium oxide and some rare-earth manganites) or a result of the mixture of ionic and electronic conductors (MIEC composite).[3] The main advantage of the MIEC composite is the possibility for tailoring the properties according to optimized parameters for a specific application.[3] In this context, the SOFC anode is the cermet ZrO_2:Y_2O_3/Ni (YSZ/Ni), produced by the reduction of the precursor composite ZrO_2:Y_2O_3/NiO (YSZ/NiO).[4] Both the cermet and the oxide precursor are MIEC composites and must fulfill several requirements for a high-performance SOFC. An important issue regarding this anode material is the reduction of the Ni volume fraction for better matching of the thermal expansion coefficient with the electrolyte, while both high electric conductivity and catalytic activity must be preserved.[4]

In fact, the final properties of the anode cermet are strongly dependent on the precursor composite, and various studies deal with the fabrication of the YSZ/NiO composite aiming for the production of SOFC anodes, but rather few papers report a more detailed microstructural and electrical characterization of the precursor composite.[5-7] The usually high temperatures ($\geqslant$1500°C) reported for the densification of the composite promote the YSZ destabilization or solid solution formation due to the reaction with NiO, resulting in a considerable reduction of the electrical conductivity.[8-10] It is well known that the electrical properties of composites depend not only on the electrical properties of each phase but also are strongly influenced by microstructural features such as grain size, distribution, and morphology. The electrical properties of composite media are an important subject, and although several proposed models like percolation and effective media are usually applied, no analytical solution for this problem has been found so far.[11,12] Moreover, the nature of the charge carriers and the dependence of the electrical transport properties on the microstructure, temperature, and oxygen partial pressure can be considered as important issues for electrochemical applications of MIEC composites.

Thus, in order to produce high-performance anodes for SOFCs, a detailed characterization of the electrical and microstructural properties of the YSZ/NiO composite prepared by a liquid mixture technique was performed. The observed high sinterability and high electrical conductivity of the studied composites can be considered as important advantages of the liquid mixture technique when compared to the ones usually reported. The main results show that the microstructure and the ionic/electronic transference numbers of high-conductivity composites can be tuned for high-temperature electrochemical applications. Moreover, an optimized microstructure of the YSZ/NiO composite is achieved after reduction of YSZ/Ni cermets, with high electrical conductivity at relatively low Ni content.

Experimental

The precursor composite $(1-v)$ (ZrO_2:8 mol % Y_2O_3)/vNiO (YSZ/vNiO) was prepared in the $0 \leqslant v(\text{vol }\%) \leqslant 100$ range and tailored to result, after reduction, in YSZ/vNi cermets with v within the range for SOFC anodes. These materials were prepared by a modified liquid mixture technique and further details can be found elsewhere.[13] Briefly, this technique consists of the evaporation of a dispersion of YSZ (Tosoh) powder in a solution of nickel acetate tetrahydrate (Carlo Erba) and ethanol, followed by calcination at 450°C/5 h to eliminate the organic material. Scanning electron microscopy (SEM) analysis of the as-produced powders revealed that the composite powders were made of a homogenous mixture of NiO nanoparticles ($d_{NiO} \approx 15$ nm) with YSZ particles ($d_{YSZ} \approx 100$ nm).[13] Pellets were formed by uniaxial pressing and sintering at 1350°C. X-ray diffraction (XRD) data were collected in a model D8 Advance Bruker-AXS diffractometer in a Bragg–Brentano θ-2θ configuration using Cu Kα radiation in the 25–85° 2θ range with step size 0.02° 2θ and 10 s counting time. Refinement of the XRD patterns was carried out by the Rietveld method using GSAS software and the reported Inorganic Crystal Structure Database (ICSD) no. 75316, 9866, and 44767 for YSZ, NiO, and Ni, respectively. The microstructure of polished and fractured surfaces of sintered samples was observed by SEM. The electrical properties of the YSZ/vNiO composite were studied by electrochemical impedance spectroscopy measurements $Z(\omega,T)$ carried out using a 4192A LF impedance analyzer in the temperature range 100–800°C and frequency range 5 Hz–13 MHz with an applied excitation signal of 200 mV. The oxygen partial pressure (p_{O_2}) was varied in the range of $1-10^{-6}$ atm using a YSZ electrochemical oxygen pump and sensor system connected to the impedance analyzer.[14] The YSZ/vNi cermets were produced by reducing the precursor composite by

* Electrochemical Society Student Member.
** Electrochemical Society Active Member.
z E-mail: cfonseca@ipen.br

heat-treating at 550°C under H_2 flow (100 mL/min) for 5 h. The microstructure of the cermets was characterized by XRD and SEM analysis. Standard four-probe dc electrical resistance $\rho(T)$ measurements of bar-cut cermets were performed in the temperature range 100–800°C under He flow using a Keithley current source and voltmeter. In all electrical measurements, Pt wires were attached to Ag contact pads painted on the surface of the samples and cured at 400°C.

Results and Discussion

Figure 1 shows the XRD patterns of the YSZ/vNiO samples. All the diffraction peaks were indexed according to the cubic structure of both oxides, space group $Fm\bar{3}m$, and no extra peaks due to any spurious phase were detected. Table I reports the main parameters of the calculated XRD patterns. The good quality of the Rietveld refinements is evidenced by the low values of the reliability factors $\chi^2 \approx 2$ and $R_{\text{Bragg}} \approx 3\%$. The calculated volume fractions of the phases are within ~3% of the nominal values, and the refined lattice parameters (a) of both oxides are in good agreement with previously reported data.[15] The YSZ lattice parameter dependence on the NiO content, displayed on the inset of Fig. 1, shows no significant changes, indicating that no appreciable solid solution occurred at 1350°C. If Ni^{2+} substitutes either for Zr^{4+} or Y^{3+} ions in the YSZ structure, a pronounced decrease in the lattice parameter would occur due to the smaller ionic radius of nickel.[5,16] It was already reported that the NiO solubility limit in the cubic zirconia structure is <5 mol % (<8 vol %) for dense samples sintered at 1600°C for 4 h.[9] In the present study, sintering the prepared powders at a relatively lower temperature resulted in dense composite samples, as inferred from the measured relative densities. The composite densities were determined by the Archimedes method and the theoretical values were calculated by the rule of mixture using the reported density values of YSZ and NiO. The apparent density of the specimens was found to be ~96% of the theoretical value.

SEM images of polished and thermally etched surfaces shown in Fig. 2 indicate that both phases are homogenously distributed in the composites. Specimens sintered at 1350°C for 1 h (Fig. 2a and b) were found to have estimated average grain size ~800 and ~700 nm for YSZ and NiO, respectively. In addition, the average grain size of both phases was observed to be nearly independent of the relative composition. The SEM images show that the average size of the NiO particles heat-treated at 450°C exhibited a large increase in size when sintered at 1350°C, while pure YSZ samples sintered under similar conditions had an average grain size comparable to those found in the YSZ/NiO composites.[17]

The microstructural characterization of the YSZ/vNiO composites revealed that the liquid mixture technique produced sinteractive powders, yielding dense samples formed by a homogeneous mixture of the oxides. The electrical properties were then investigated by impedance spectroscopy measurements. The $Z(\omega,T)$ data showed at least two semicircles in the whole frequency and temperature ranges studied.[18] However, in this study the focus was on the total electrical resistance of the YSZ/vNiO composite, which was obtained by fitting the low-frequency end of the impedance diagrams. The electrical conductivity $\sigma(T)$ of the composites was measured in a wide range of temperature, and Fig. 3 shows the $\sigma(T)$ dependence on the NiO content.

In addition, the transport mechanism of the composite was studied with the Arrhenius plots, shown in Fig. 4. As far as the electrical transport is concerned, YSZ is known to be an ionic conductor (ionic transference number $t_I \approx 1$) with thermally activated transport of oxygen vacancies with an activation energy $\Delta E \approx 1$ eV over a wide range of both temperature and oxygen partial pressure (p_{O_2}).[4] NiO is a p-type semiconductor, the charge carriers being the electron holes due to Ni vacancies.[5,19] NiO exhibits a discontinuity in the Arrhenius plots at a temperature close to the Néel temperature ($T_N \approx 250$°C), and the activation energies are $\Delta E \approx 0.7$ and 0.3 eV for $T < T_N$ and $T > T_N$, respectively.[5,19] The $\sigma(T)$ data at low temperatures ($T < 400$°C) shown in Fig. 3 indicated that the NiO content had a large influence on the electrical conductivity of the composite. At low temperatures, YSZ behaved as insulating particles and the $\sigma(T)$ increased three orders of magnitude from v = 0–23 vol % at $T \approx 240$°C. This remarkable increase of $\sigma(T)$ is due to the increase in the density of electronic charge carriers from NiO and indicates that the percolation threshold was attained at $v \approx 20$ vol %. The relatively low critical volume fraction may be attributed to the high dispersion and good connectivity of NiO par-

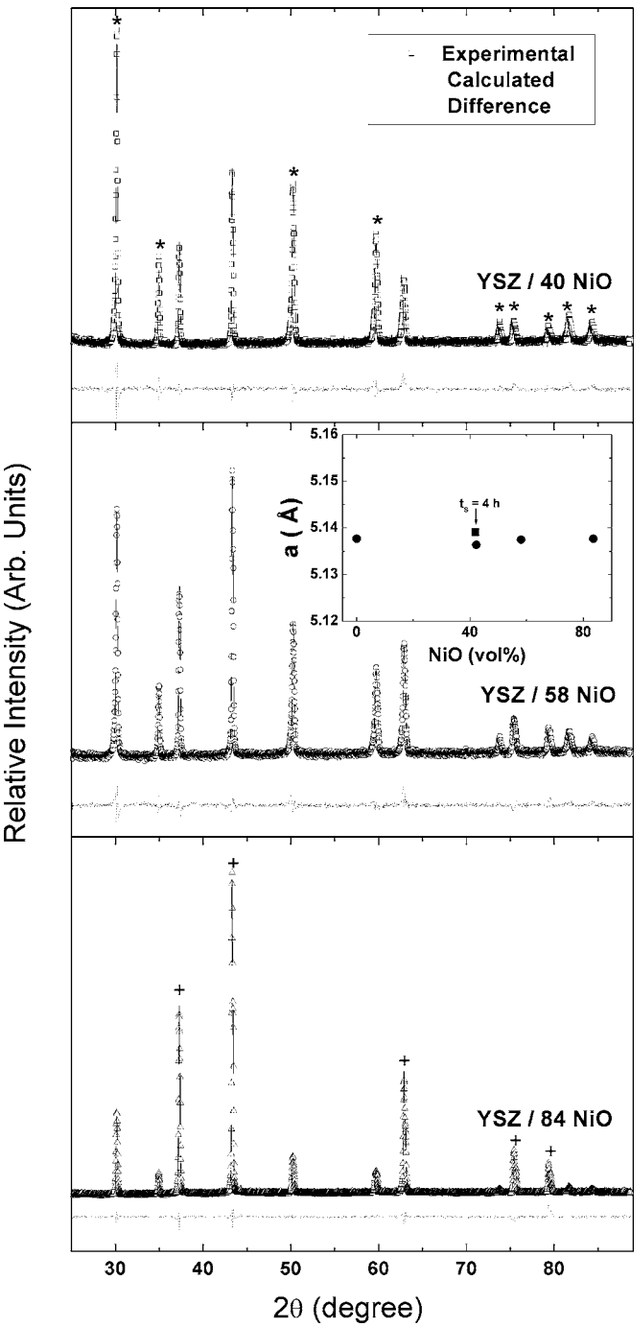

Figure 1. XRD patterns of $(1 - v)$ (ZrO_2:8 mol % Y_2O_3)/v NiO samples with v = 40, 58, and 84 vol %. The * and + symbols indicate the YSZ and NiO main diffraction peaks, respectively. The experimental, calculated, and difference plots are shown. The inset shows the dependence of the calculated lattice parameter of cubic zirconia on the NiO content.

Table I. Rietveld refined parameters of the YSZ/NiO composite. The atomic positions and thermal factors were fixed according to the values reported in the crystallographic files. ICSD no. 75316 (YSZ) and 9866 (NiO).

Nominal NiO (vol %)	YSZ a (Å)	NiO a (Å)	χ^2	R_{Bragg}	Calculated NiO (vol %)
40	5.1364(1)	4.1888(1)	2.7	4.0	41.5(2)
58	5.1375(1)	4.1886(1)	2.2	3.5	55.1(1)
84	5.1377(1)	4.1790(1)	2.3	3.4	84.9(1)

ticles in the YSZ matrix, as well as to the average grain size ratio of the two phases.[12] It is interesting that the usually observed decrease in the electrical conductivity at low NiO content ($v \leqslant 10$ vol %), ascribed to solid solution formation of YSZ/NiO composites sintered at higher temperatures, is absent in the samples prepared by the liquid mixture technique.[5] As the NiO percolation threshold was attained at $v \approx 20$ vol %, the electrical transport of the specimens with $v < 20$ vol % is dominated by the ionic charge carriers of YSZ. In fact, the Arrhenius plots show that samples with $v < 20$ vol % exhibited a single thermally activated process in the whole temperature range with $\Delta E \approx 1$ eV (Fig. 4). However, samples with $v \approx 16$ vol % showed $\Delta E \approx 0.7$ eV, a value appreciably lower than the one of pure YSZ ionic conductor, as observed in Fig. 4.[5] At $v = 23$ vol % the discontinuity of the Arrhenius plot at $T_N \approx 250$°C was observed as a signature of the NiO transport behavior, further confirming the percolation of the semiconductor phase in the ionic matrix and indicating that samples with $v \approx 20$ vol % have mixed conductivity. Samples with $v \geqslant 20$ vol % have ΔE close to the values previously reported for NiO in the two temperature ranges (0.7 eV for $T < T_N$ and 0.3 eV for $T > T_N$), as shown in Fig. 4. Further increasing the NiO content up to $v \approx 60$ vol % resulted in increasing the electrical conductivity; the electrical transport properties of the samples in the $20 < v < 60$ vol % range are believed to be due to both the ionic

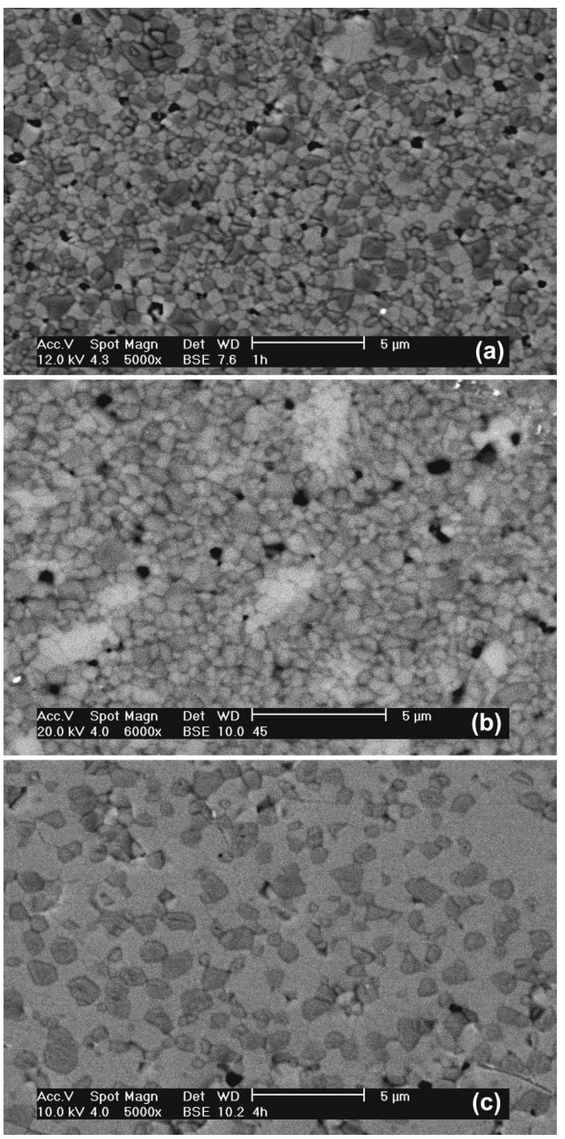

Figure 2. Backscattered SEM images of the $(1 - v)$ $(ZrO_2$:8 mol % $Y_2O_3)/v$ NiO samples with $v = 40$ (a) and 58 (b) sintered at 1350°C/1 h, and $v = 40$ (c) sintered at 1350°C/4 h. The darker grains correspond to the NiO.

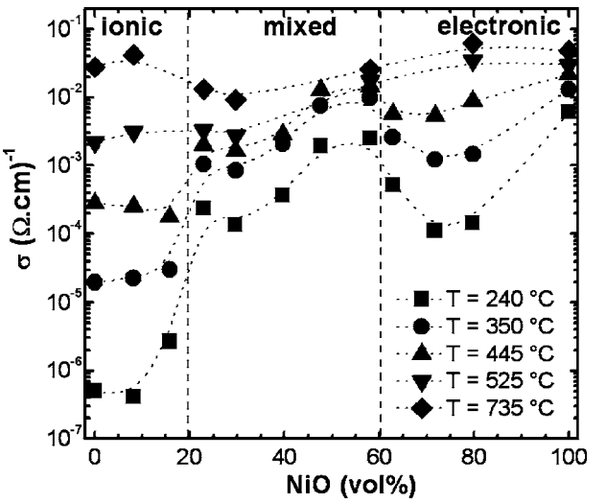

Figure 3. Electrical conductivity dependence on NiO content of $(1 - v)$ $(ZrO_2$:8 mol % $Y_2O_3)/v$ NiO composite measured at different temperatures. The lines are guide for the eye.

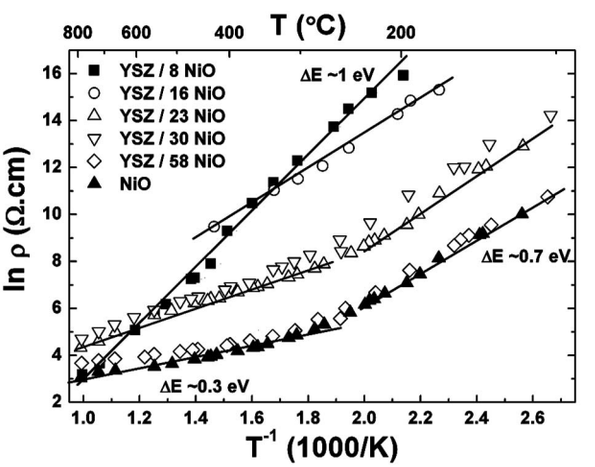

Figure 4. Arrhenius plots of the $(1 - v)$ $(ZrO_2$:8 mol % $Y_2O_3)/v$ NiO composites.

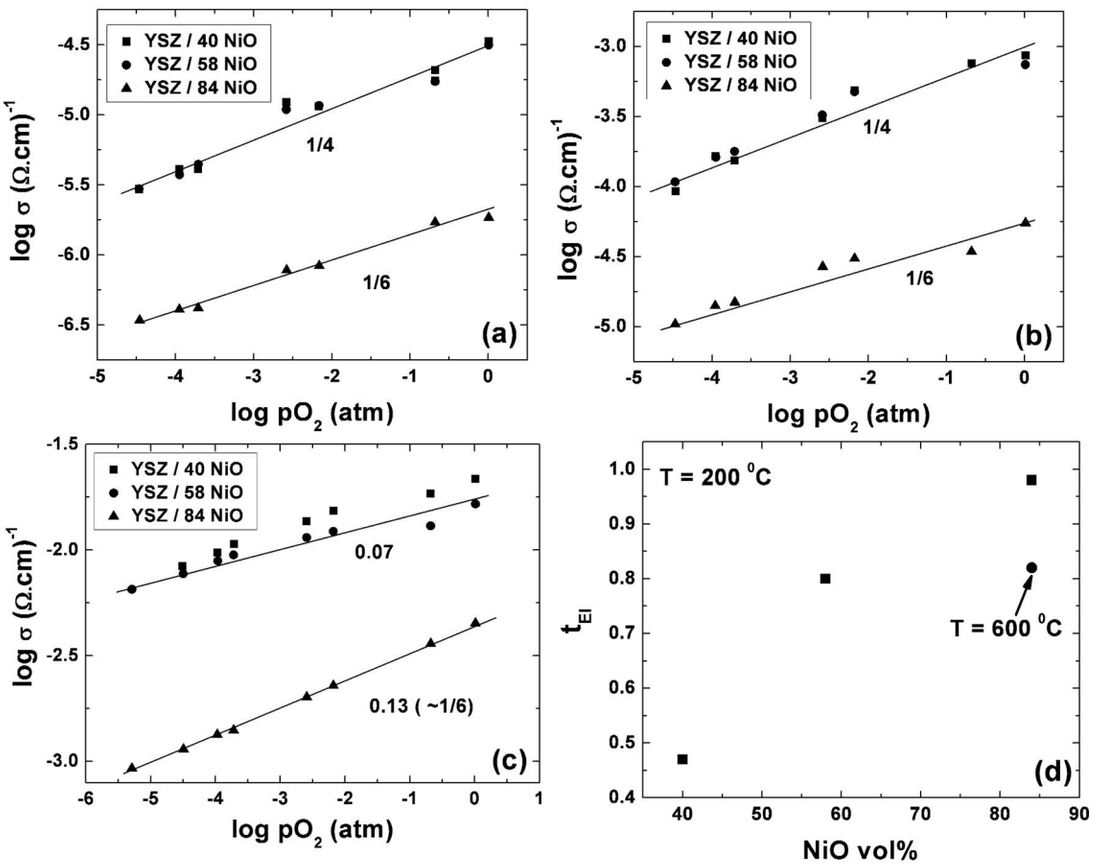

Figure 5. Electrical conductivity dependence on the oxygen partial pressure of $(1 - v)$ ZrO_2:8 mol % Y_2O_3/v NiO composites with v = 40, 58, and 84 vol %, measured at 200°C (a), 300°C (b), and 600°C (c), and electronic transfer number dependence on the NiO content (d).

and electronic charge carriers, as observed at low temperatures ($T < 400$°C) in Fig. 3. The electrical transport data suggest that the enhanced NiO connectivity in the YSZ/NiO composites, prepared by the liquid mixture technique, lead to electronic pathways at relatively lower semiconductor content than in other reported samples.[7] Specimens with NiO content $v > 60$ vol % exhibited a decrease in the electrical conductivity down to a minimum at $v \approx 80$ vol %. In these specimens with large NiO content the transport was mainly due to the electron holes, while YSZ grains acted as insulating inclusions at low temperatures. However, the transport properties of the composites were strongly affected by the temperature due to the different activation energies of the electronic ($\sim$0.3 eV) and ionic ($\sim$1 eV) conductors at high temperatures. With increasing temperature, the higher ΔE value of YSZ promoted a high conductivity of the O^{2-} ions, and $\sigma(T > 500$°C) of the composite samples were of the same order of magnitude in the whole NiO concentration range. In fact, samples with $v < 20$ vol % and $v > 60$ vol % exhibited the most pronounced increase in the electrical conductivity with increasing temperature, while samples in the mixed transport range were considerably less influenced by temperature (Fig. 3).

The combined results shown in Fig. 3 and 4 allowed us to estimate three different transport characteristics of the YSZ/vNiO composites: for $v < 20$ vol % the composites were essentially ionic conductors, for $20 < v < 60$ vol % the composites were MIECs, and for $v > 60$ vol % the transport was predominately due to electron holes.[6,18] This behavior was further confirmed by the analysis of the electrical conductivity data taken under different oxygen partial pressures. Figure 5a-c shows the electrical conductivity dependence on the p_{O_2} of v = 40, 58, and 84 vol % samples measured at 200, 300, and 600°C, respectively. These findings demonstrated that the samples exhibited the expected linear behavior of a p-type semiconductor. In addition, by assuming that the phases are connected in parallel for NiO concentrations above the percolation threshold, the linear dependence of σ on the p_{O_2} was fitted according to the relation $\sigma = A + B\, p_{O_2}^{x}$, where A is the p_{O_2}-independent ionic conduction, B is the electronic conduction, and x is the exponent giving the

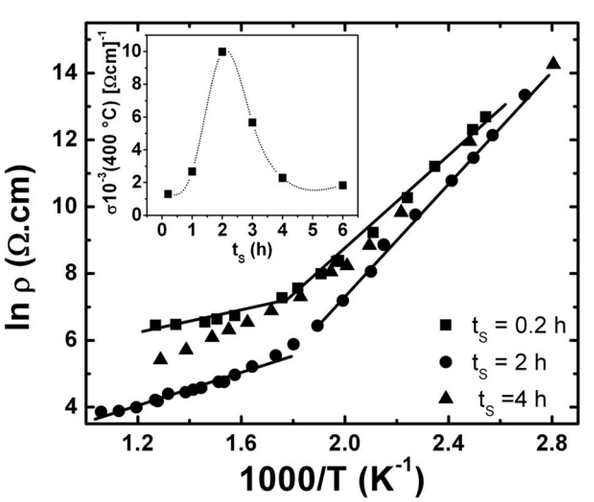

Figure 6. Arrhenius plots of the (ZrO_2:8 mol % Y_2O_3)/40 vol % NiO composite sintered at 1350°C for different times. The inset shows the dependence of the electrical conductivity measured at 400°C on the sintering time.

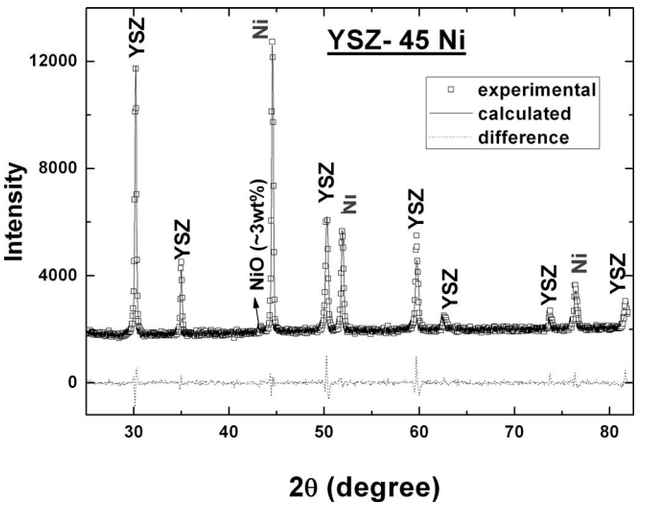

Figure 7. Experimental and calculated XRD patterns of the reduced cermet (ZrO_2:8 mol % Y_2O_3)/45 vol % Ni and the difference plot.

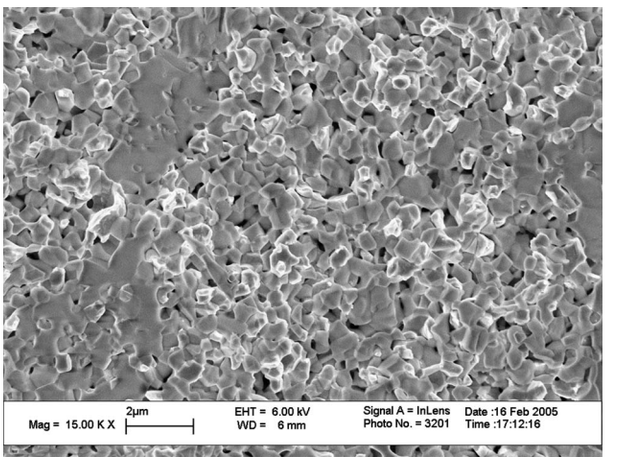

Figure 8. SEM of the fractured surface of the (ZrO_2:8 mol % Y_2O_3)/28 vol % Ni sintered for 2 h.

p_{O_2} dependence of the semiconductor phase. For measuring temperatures 200 and 300°C, both samples $v = 40$ and 58 vol % had a $p_{O_2}^{1/4}$-dependence and the $v = 84$ vol % sample exhibited a less pronounced p_{O_2} dependence, being the fitted exponent $x = 1/6$. The electronic transport in NiO has been already studied, and both p_{O_2} dependences 1/4 and 1/6 have been measured. It has been reported that the exponent x depends on the ionization state of the Ni vacancies.[20] When the concentration of single-ionized Ni vacancies is larger than the double-ionized one, the p_{O_2} dependence is 1/4, and when double-ionized vacancies predominate, the electron hole concentration is proportional to $p_{O_2}^{1/6}$. In fact, high-purity NiO single crystals were found to have a $p_{O_2}^{1/6}$ dependence and for less pure NiO specimens a 1/4 power has been observed.[20] Thus, the results here presented suggested that the samples with high NiO content have a higher content of doubly-charged Ni vacancies and the mixture with YSZ seems to yield a p_{O_2} dependence close to the 1/4 power, in agreement with previously reported data.[5] Increasing the measuring temperature up to 600°C caused a decrease in the electrical conductivity dependence on the p_{O_2}, and the fitted exponents were lower than those found at low temperatures (Fig. 5c). Such an effect was more pronounced in samples with larger amounts of the ionic phase and indicates that the effective fraction of ionic charge carriers increased when the thermal energy activated the p_{O_2}-independent transport of the YSZ oxygen ions, in agreement with the results of Fig. 3. The electronic transfer number t_{El} was estimated by using $t_{El} = 1 - t_I = Bp_{O_2}^x/\sigma$; Fig. 5d shows the t_{El} values measured at 200°C. As expected, increasing the NiO content increased the electronic transport from $t_{El} \approx 45$–98% for the samples $v = 40$ and 84 vol %, respectively, further indicating the mixed conduction of the samples in the $20 < v < 60$ vol % range and the predominant electronic conduction in the sample $v = 84$ vol %. In addition, for increasing temperatures, the electronic transfer number decreased, and at 600°C the t_{El} of the sample $v = 84$ vol % decreased from ~98 to 80%, indicating that the transport due to O^{-2} in YSZ became relevant at high temperatures even for relatively low volume fraction (YSZ ≈ 16 vol %). The above results indicated that both the relative phase volume fraction and the temperature play important roles in the transport properties of the YSZ/NiO composites.

The microstructure is also considered important for determining the transport properties of a composite. Thus, to further evaluate the electrical properties in the mixed conduction range, YSZ/NiO specimens were sintered at 1350°C for different sintering times, t_S. Samples with $v = 40$ and 58 vol % were sintered at 1350°C for $0.2 \text{ h} \leqslant t_S \leqslant 6$ h; the discussion is here focused on the $v = 40$ vol % sample, which is close to the percolation threshold and exhibited a more pronounced dependence on t_S. The XRD data show that the YSZ lattice parameters did not depend on the sintering time, further indicating that no solid solution between the oxides occurred at 1350°C (see inset of Fig. 1). The relative density was found to continuously increase from ~82 to ~97% of the theoretical value when the sintering time t_S increased from 0.2 to 2 h,

Table II. Rietveld refined parameters of the reduced cermets. The atomic positions and thermal factors were fixed according to the values reported in the crystallographic files ICSD no. 75316 (YSZ) and 44767 (Ni).

Nominal Ni (vol %)	YSZ a (Å)	Ni a (Å)	χ^2	R_{Bragg}	Calculated Ni (vol %)
28	5.1402(1)	3.5274(1)	2.1	3.1	28.2(3)
45	5.1405(1)	3.5277(1)	3.2	3.8	40.3(2)

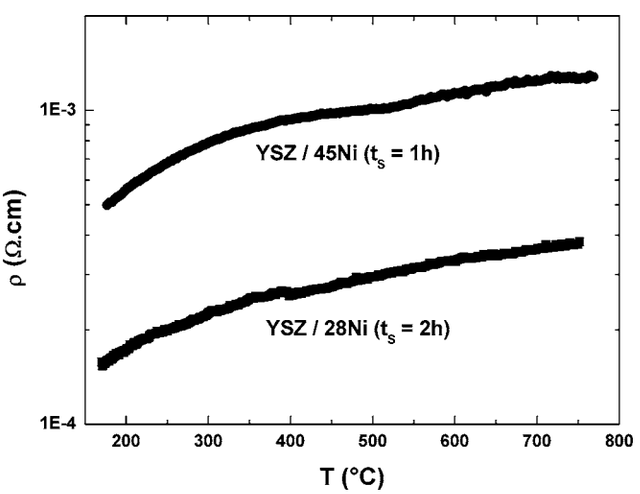

Figure 9. dc electrical resistivity dependence on temperature for the (ZrO_2:8 mol % Y_2O_3)/v Ni cermets for $v = 28$ and 45 vol % sintered for 2 and 1 h, respectively.

Table III. Estimated values of NiO and Ni relative volume fraction, electrical conductivity, and the respective measuring temperatures of YSZ/NiO (Ni) composites prepared by different methods reported in the literature.

NiO (vol %)	Ni (vol %)	Preparation method	σ $(\Omega\ \text{cm})^{-1}$	T (°C)	Reference
23	—	Modified liquid mixture	3.3×10^{-3}	450	This work
25	—	Aqueous coassembly	2.9×10^{-5}	450	7
40	—	Modified liquid mixture	9.1×10^{-3}	400	This work
40	—	Solid-state mixture	6.3×10^{-5}	400	5
48	—	Modified liquid mixture	1.3×10^{-2}	450	This work
52	—	Modified Pechini	2.0×10^{-4}	450	21
—	28	Modified liquid mixture	2.8×10^{3}	700	This work
—	30	Combustion synthesis	77	700	8
—	~27	Polymer precursors	3.4×10^{2}	700	23
—	40	Coat-mix	from 78 to 4.0×10^{3}	800	24

while for $t_S \geqslant 2$ h the relative density remained nearly constant. The SEM images revealed that increasing t_S increased the average grain size of both YSZ and NiO, being ~1.5 and ~1.2 μm, respectively, as displayed in Fig. 2c. It was already reported that NiO particles may inhibit YSZ grain growth; however, probably due to the initial average particle size of the powders produced by the liquid mixture technique, such an effect was not observed.[21] By comparing the SEM images of the samples sintered for 1 and 4 h (Fig. 2a and c), it is important to observe that increasing t_S resulted in a larger separation between NiO grains. The microstructural features of the isothermal sintering at 1350°C have a strong influence on the electrical properties, as observed in Fig. 6. The Arrhenius plots of the samples with v = 40 vol % sintered for different times exhibited the same behavior previously discussed; however, at high temperatures ($T > T_N$) a significant dependence on the sintering time was observed (see inset of Fig. 6). The electrical conductivity σ(T = 400°C) increased with increasing t_S up to 2 h, reaching a maximum due to the decrease in porosity. Further increasing $t_S > 2$ h resulted in a decrease of σ of an order of magnitude, which may be correlated with the larger separation of NiO grains observed in Fig. 2. This finding evidenced that the percolation of charge carriers in MIEC composites can also be controlled by the relative grain size of both phases.

In order to investigate the suitability of the liquid mixture technique and the influence of the precursor composite properties on the SOFC anode cermet, the composites in the mixed conduction region with 40 and 58 vol % NiO and sintered for t_S = 2 and 1 h, respectively, were reduced under H_2 flow at 550°C. The resulting cermets with nominal Ni content 28 and 45 vol % were analyzed by XRD, as shown in Fig. 7. The XRD data were refined by the Rietveld method, and Table II reports the main calculated parameters. The calculated lattice parameters of both phases are similar to the values reported in the literature, and the Ni volume fractions estimated were slightly smaller than the nominal values. This might be due to the relatively low temperature used in the reduction that resulted in a small fraction of remaining NiO (≤3 wt %, as inferred from Rietveld refinements) in the cermet. Figure 8 shows, as an example of the microstructure of the reduced samples, a representative region of a typical fractured surface of the YSZ/28 Ni cermet sintered for 2 h. It is possible to observe that the reduction at 550°C did not cause any significant increase in the particle size of the metallic phase (brighter regions in Fig. 8) when compared to the NiO particles (darker regions in Fig. 2). In addition, this micrograph suggests the presence of a larger porosity (cf. Fig. 2) resulting from the NiO reduction. However, a clear percolation path of the metallic phase was seen through the sample, as inferred from the electrical properties of the cermet. Figure 9 shows the temperature dependence of the electrical resistivity of the samples with 28 and 45 vol % Ni sintered for 2 and 1 h, respectively. The electrical resistivity data exhibited essentially the same behavior as pure Ni, with the characteristic change of slope associated with the Curie temperature at $T \approx 350$°C, but shifted to higher resistivity values due to the presence of both YSZ and pores.[22] However, both samples showed larger values of electrical conductivity at lower Ni concentrations than data usually reported for this cermet.[8,23,24] In addition, the cermet with 28 vol % Ni (former v = 40 vol % NiO) had smaller electrical resistivity values, attributed to both the higher electrical conductivity of the precursor composite and to the lower porosity after reduction of samples with lower volume fraction of NiO. These results confirmed that the control of the microstructural properties of the precursor composite is an important factor to produce cermets with high electrical conductivity at low Ni contents.

For comparison purposes, the present electrical conductivity values along with reported ones for YSZ/NiO composites and YSZ/Ni cermets prepared by other techniques are displayed in Table III. The differences observed in the data referenced in Table III can be ascribed to the strong dependence of the electrical conductivity on the preparation method. In order to attain high density, sintering temperatures higher than the ones used in this work are usually required. Sintering at higher temperatures is likely to promote the formation of solid solution between the oxides, which is expected to result in lower values of the electrical conductivity.

Conclusions

In summary, YSZ/NiO composites have been prepared by a liquid mixture method, which resulted in homogenous powders with high sinterability. The relatively low sintering temperature inhibited solid solution formation between the two oxides. The NiO concentration ranges where the main charge carriers are ionic, mixed, and electronic were estimated. The effectiveness of the described preparation method is evidenced by the high values of both the relative density and the electrical conductivity of the composites at low NiO contents, indicating the good connectivity of the semiconductor particles. The results show that the careful design of a mixed ionic–electronic composite for optimized transport properties must take into consideration the relative composition of the phases, the microstructural features, and operation temperature of the electrochemical device. The suitable design of the YSZ/NiO composite allowed for the preparation of cermets with relatively low concentration of Ni and high electrical conductivity, which is an important feature concerning the application of this cermet as SOFC anodes.

Acknowledgments

This work was partially supported by the Brazilian agencies FAPESP (98/14324-0, 99/10798-0, and 03/08793-8) and CNPq (306496/88-7, 300934/94-7, 301661/2004-9); and by the Italian Ministry of Education, University and Research (MIUR) under the framework of an FISR project. Thanks are also due to Dr. E. V. Spinacé (IPEN) and Dr. R. F. Jardim (IF-USP) who helped with the cermet fabrication and dc electrical measurements, respectively.

Fundação de Amparo à Pesquisa do Estado de São Paulo assisted in meeting the publication costs of this article.

References

1. P. Knauth and H. L. Tuller, *J. Am. Ceram. Soc.*, **85**, 1654 (2002).
2. A. Thursfield and I. S. Metcalfe, *J. Mater. Chem.*, **14**, 2475 (2004).
3. I. Reiss, *Solid State Ionics*, **157**, 1 (2003).
4. N. Q. Minh, *J. Am. Ceram. Soc.*, **76**, 563 (1993).
5. Y. M. Park and G. M. Choi, *J. Electrochem. Soc.*, **146**, 883 (1999).
6. Y. M. Park and G. M. Choi, *Solid State Ionics*, **120**, 265 (1999).
7. M. Mamak, N. Coombs, and G. Ozin, *Adv. Funct. Mater.*, **11**, 59 (2001).
8. U. Anselmi-Tamburini, G. Chiodelli, M. Arimondi, F. Maglia, G. Spinolo, and Z. A. Munir, *Solid State Ionics*, **110**, 35 (1998).
9. A. Kuzjukevics and S. Linderoth, *Solid State Ionics*, **93**, 255 (1997).
10. H. Kondo, T. Sekino, T. Kusunose, T. Nakayama, Y. Yamamoto, and K. Niihara, *Mater. Lett.*, **57**, 1624 (2003).
11. N. F. Uvarov, *Solid State Ionics*, **136**, 1267 (2000).
12. D. S. McLachlan, M. Blaszkiewicz, and R. E. Newnham, *J. Am. Ceram. Soc.*, **73**, 2187 (1990).
13. V. Esposito, C. D'Ottavi, S. Ferrari, S. Licoccia, and E. Traversa, in *SOFC-VIII*, S. C. Singhal and M. Dokiya, Editors, PV 2003–07, p. 643, The Electrochemical Society Proceedings Series, Pennington, NJ (2003).
14. M. C. Steil, F. C. Fonseca, Y. V. França, J. F. Q. Rey, E. N. S. Muccillo, and R. Muccillo, *Ceramica (Sao Paulo, Braz.)*, **48**, 146 (2002).
15. R. P. Ingel and D. Lewis III, *J. Am. Ceram. Soc.*, **69**, 325 (1986).
16. R. D. Shannon, *Acta Crystallogr., Sect. A: Cryst. Phys., Diffr., Theor. Gen. Crystallogr.*, **A32**, 751 (1976).
17. F. C. Fonseca and R. Muccillo, *Solid State Ionics*, **131**, 301 (2000).
18. V. Esposito, D. Z. de Florio, F. C. Fonseca, E. N. S. Muccillo, R. Muccillo, and E. Traversa, *J. Eur. Ceram. Soc.*, **25**, 2637 (2005).
19. M. W. Vernon and M. C. Lovell, *J. Phys. Chem. Solids*, **27**, 1125 (1966).
20. C. M. Osburn and R. W. West, *J. Phys. Chem. Solids*, **32**, 1331 (1971).
21. P. Durán, J. Tartaj, F. Capel, and C. Moure, *J. Eur. Ceram. Soc.*, **23**, 2125 (2003).
22. L. Gmelin, *Gmelin Handbuch Der Anorganischen Chemie*, Ni [A II], p. 355, Springer-Verlag, New York (1974).
23. V. Petrovsky, T. Suzuki, P. Jasinski, and H. U. Anderson, *Electrochem. Solid-State Lett.*, **8**, A341 (2005).
24. F. Tietz, F. J. Dias, D. Simwonis, and D. Stöver, *J. Eur. Ceram. Soc.*, **20**, 1023 (2000).